

スラブ流体は塩水 Slab-fluids contain chlorine

川本 竜彦^{1*}
KAWAMOTO, Tatsuhiko^{1*}

¹ 京都大、理・地球熱学
¹Institute for Geothermal Sciences, Kyoto University

スラブ流体が塩水である可能性は高いと提案する。根拠の一つは天然の岩石中に含まれる流体包有物である。沈み込み帯のマントル捕獲岩中の塩濃度としてピナツボ火山のマントル捕獲岩中に 5.1 重量%の塩水を発見した (Kawamoto ほか、2013、PNAS)。続いて、一ノ目瀉火山のマントル捕獲岩中に 3.7 重量%の塩水を発見した (Kumagai ほか、投稿中) ほか、多くの共同研究者と塩水の流体包有物を記載し続けている。これまで観察した H₂O にとむ流体包有物は多かれ少なかれ必ず塩水である。このことから、スラブ流体は塩素を含んでいると考える。

スラブ流体が塩水であることは、沈み込み帯での元素移動にどのような影響を持つか考えたい。そこで、多くの共同研究者達と、メルトと水流体の間の元素分配実験を放射光実験設備で行い、塩濃度が与える影響を理解しつつある。その結果、スラブ流体は塩水だと考えると、島弧玄武岩の微量成分元素の特徴を定性的に説明することが可能であると提案する。ただし、定量的には、まだよくわかっていない。それは、塩素を含んだ超臨界流体が塩水とメルトに分離し、それぞれがマグマを作ると提案している (Kawamoto ほか、2012、PNAS) が、再びおたがいに混ざったりする過程は複雑で、どのような元素のマグマになるか予想することが困難であることが主な原因である。もう一つは、実験に使用した塩水の濃度は天然の流体包有物で確認されている塩濃度の倍から 5 倍である。実験では濃い塩水とマグマの間には不混和があると考えているが、5%の場合、塩水とマグマの間の混和・不混和領域がどのようになるかさえ、まだわかっていない。

参考文献

Kawamoto T., Kanzaki M., Mibe K., Matsukage K.N., Ono S. (2012) Separation of supercritical slab-fluids to form aqueous fluid and melt components in subduction zone magmatism. *Proc. Nat. Acad. Sci. USA* 109, 18695-18700.

Kawamoto T., Yoshikawa M., Kumagai Y., Mirabueno M.H.T., Okuno M., Kobayashi T. (2013) Mantle wedge infiltrated with saline fluids from dehydration and decarbonation of subducting slab. *Proc. Nat. Acad. Sci. USA* 110, 9663-9668.

キーワード: 沈み込み帯, H₂O, 流体包有物, マントルウェッジ, 放射光 X 線, マグマ
Keywords: subduction zone, H₂O, fluid inclusion, mantle wedge, synchrotron X-ray, magma

岩石-水反応の数値モデリング～表層環境を中心として～ Numerical modeling of water-rock reaction with a focus on the earth's surface environment

横山 正^{1*}
YOKOYAMA, Tadashi^{1*}

¹ 大阪大学理学研究科宇宙地球科学専攻

¹ Osaka University, Graduate School of Science, Department of Earth and Space Science

岩石-水反応は、岩石内部における溶解・沈殿等の反応と元素の拡散や水の移流との相互作用により進行する。岩石内部の反応・輸送過程は、以下の式で定量的に記述できる：

$$\phi(\partial c/\partial t) = D_e(\partial^2 c/\partial x^2) - v\phi(\partial c/\partial x) + Ar_0f(c)$$

この式は一次元の反応・輸送方程式の一例であり、 c は溶液中の元素濃度 (mol/cm³)、 t は時間 (s)、 x は距離 (cm) (地表面からの深さなど)、 ϕ は間隙率 (無次元)、 D_e は有効拡散係数 (cm²/s)、 v は間隙水の流速 (cm/s)、 A は岩石の単位体積あたりの表面積 (cm²/cm³)、 r_0 は鉱物の溶解速度定数 (mol/cm²/s)である。 $f(c)$ は溶解速度の溶存元素濃度依存性を表す関数であり、石英など溶存 Si 濃度の増加に比例して溶解速度が下がる鉱物の場合は、 $f(c)=(1-c/c_{eq})$ となる (c_{eq} は鉱物の平衡濃度 (mol/cm³)) (Schott et al., 2009)。反応・輸送方程式を解くことにより、岩石内部の溶存元素濃度と溶解速度の分布や、一次鉱物と二次鉱物の分布がどのように時間変化するかなどの情報が得られる。そのような解析は反応・輸送モデリングと呼ばれ、土壌の生成 (Maher et al., 2009) や CO₂ の地下貯留に伴う反応 (Xu et al., 2010) など、様々な過程の研究に応用されている。

反応・輸送方程式で用いる各パラメータの値は、フィールドでの実測、室内実験、モデリングにおけるフィッティング (計算結果と天然の産状の比較) などにより見積もられる。反応・輸送モデリングで天然の現象を正確に再現するためには、個々のパラメータの値をできるだけ正確に見積もることが基本になる。しかし、どのような値を設定すれば適切なモデリングになるかの判断は難しい。例えば、反応表面積 A については、鉱物へのガスの吸着量から求めた値や、鉱物の外形を球などと近似して得られる表面積がよく用いられるが、それらの表面のどれだけの割合が実際に反応に寄与しているかは不明な場合が多い。また、一つの鉱物に対して様々な $f(c)$ が提案されていたり、溶解速度の時間変化 (White and Brantely, 2003) が生じたりするため、採用すべき反応速度則がよく分からない場合もある。したがって、適切なパラメータの設定の方法は、主要な研究課題の一つである。

地球表層環境の岩石-水反応においては、岩石内部で水の浸透や乾燥が断続的に起こり、それに伴って間隙を水が満たす割合 (水飽和率) が変化するため、その影響の評価は重要である。水飽和率が下がると、岩石内部の水の通りやすさ (透水係数) や有効拡散係数 D_e が低下し、モデリングの結果に大きく影響することが示されている (Yokoyama, 2013)。また、水飽和率が反応表面積 A にどのような影響を及ぼすかも近年明らかになってきている (Nishiyama and Yokoyama, 2013)。

キーワード: 反応・輸送モデリング, 岩石-水反応

Keywords: Reactive transport modeling, Water-rock reaction

地殻におけるシリカ析出の反応速度 Kinetics of overall silica precipitation within the Earth's crust

最首 花恵^{1*}; 岡本 敦²; 土屋 範芳²
SAISHU, Hanae^{1*}; OKAMOTO, Atsushi²; TSUCHIYA, Noriyoshi²

¹ 独立行政法人産業技術総合研究所, ² 東北大学大学院環境科学研究科
¹ AIST, ² Tohoku University

The kinetics of dissolution and precipitation of silica minerals is important to reveal the geochemical reaction and to estimate how long silica deposits forms in the Earth's crust. The present kinetic equation for silica-water reactions was determined at 0-300 C and in the low Si saturated solution, where quartz growth on quartz surfaces occurs than that of nucleation of silica polymorphs [1]. However, the precipitation experiments of the high Si supersaturated solution showed that the co-precipitation of silica polymorphs via nucleation could occur [2], and the euhedral quartz crystals precipitates without precursor of silica polymorphs from the solution with minor components (Al and Na) [3].

In this study, the overall precipitation rate of silica minerals, which includes surface reaction of quartz (first term) and nucleation of silica polymorphs (second term), is derived empirically to estimate the total amount of silica precipitation within the Earth's crust. The previous kinetic equation of surface reaction [1] is applied as the first term. Based on the precipitation experiments of flow rate, the nucleation-controlled precipitation of silica minerals is expressed in a first order rate equation in the second term. The applicability of the nucleation term determined as the nucleation parameter is only in the conditions that precipitation occurs: in the solution supersaturated with respect to quartz, and in the supercritical conditions of water. The rate constant of nucleation is derived as a function of Al concentration in the solution based on the experiments of silica precipitation [3].

By using the new kinetic equation, silica-water interaction was simulated at the well WD-1a of the Kakkonda geothermal field, Japan, which penetrated the boundary of the hydrothermal convection and heat conduction zones [4]. Amount of dissolution and precipitation of silica minerals increases with decreasing of the fracture permeability. The largest amount of silica precipitation occurs in the downflow fluid at the permeable-impermeable boundary regardless of the fracture permeability.

The equilibrium consideration [5] and the kinetic results indicate that, if open fractures forms at the depth of the permeable-impermeable boundary, the impermeable zone could be reproduced by precipitation of silica minerals, which cause the sustainable division between the permeable zone and the impermeable zone in the Earth's crust.

References

- [1] Rimstidt and Barnes (1980) *Geochim. Cosmochim. Acta*, **44**, 1683-1699.
- [2] Okamoto et al. (2010) *Geochim. Cosmochim. Acta*, **74**, 3692-3706.
- [3] Saishu et al. (2012) *Am. Min.*, **97**, 2060-2063.
- [4] Doi et al. (1998) *Geothermics*, **27**, 663-690.
- [5] Saishu et al. (in press) *Terra Nova*.

キーワード: シリカ鉱物析出反応, 熱水実験, 反応速度式, 核形成, 透水不透水境界

Keywords: Silica precipitation, Hydrothermal experiment, Kinetic equation, Nucleation, Permeable-impermeable boundary

ハロゲンと希ガスから明らかになった堆積物中間隙水起源のマントルウェッジ中流体 Sedimentary pore-fluid origin of H₂O-rich fluid in mantle wedge revealed by halogens and noble gases

小林 真大^{1*}; 角野 浩史¹; 長尾 敬介¹; 石丸 聡子²; 荒井 章司³; 芳川 雅子⁴; 川本 竜彦⁴; 熊谷 仁孝⁴; 小林 哲夫⁵
KOBAYASHI, Masahiro^{1*}; SUMINO, Hirochika¹; NAGAO, Keisuke¹; ISHIMARU, Satoko²; ARAI, Shoji³; YOSHIKAWA, Masako⁴; KAWAMOTO, Tatsuhiko⁴; KUMAGAI, Yoshitaka⁴; KOBAYASHI, Tetsuo⁵

¹ 東京大学地殻化学実験施設, ² 熊本大学理学部地球環境科学講座, ³ 金沢大学理工学域地球学コース, ⁴ 京都大学理学研究科地球熱学, ⁵ 鹿児島大学理学部地球環境

¹GCRC, Univ. Tokyo, ²Dept. Earth Environ. Sci., Kumamoto Univ., ³Dept. Earth Sci., Kanazawa Univ., ⁴Inst. Geothermal Sci., Kyoto Univ., ⁵Dept. Earth Environ. Sci., Kagoshima Univ.

H₂O plays an important role in mantle processes in subduction zones. Yet its subducting processes to the mantle remain unknown because of scarcity of direct observations of H₂O in mantle-derived materials. Since halogen and noble gas are strongly partitioned into fluids and they show distinct elemental and/or isotopic ratios depending on their origins, their compositions in mantle rocks can provide complementary constraints on the behavior and origin of H₂O in the mantle. Although only few researches have been conducted, the subduction of halogens and noble gases derived from sedimentary pore fluids (seawater trapped in pores of deep-sea sediments) has been suggested. Pore fluid-like halogens and noble gases were found in mantle wedge peridotites which captured H₂O-rich fluids just above a subducting slab [1]. H₂O-rich fluid inclusions whose salinity is similar to that of pore fluids (salinity of pore fluids is the same level as that of seawater [2]) are found in a mantle xenolith from a subduction zone [3]. We investigated halogen and noble gas compositions of mantle wedge peridotites from subduction zones to better constrain how far the influence of subducted sedimentary pore fluids extends into the mantle.

The samples studied are harzburgitic xenoliths from the Avacha volcano in Kamchatka and the Pinatubo volcano in the Philippines, and alpine-type peridotite from the Horoman massif in Japan. H₂O-rich fluid inclusions have been found in olivine of those mantle peridotites [3,4,5].

We applied the noble gas method, in which halogens (Cl, Br, and I) are converted to corresponding isotopes of Ar, Kr, and Xe by neutron irradiation in a nuclear reactor and then the concentrations of noble gas isotopes are determined by noble gas mass spectrometry. Halogen detection limits of this method are from two to five orders of magnitude lower than conventional method, which enable to determine the low halogen abundances in mantle-derived materials. By crushing samples under ultra-high vacuum, noble gases are selectively extracted from H₂O-rich fluid inclusions. Unirradiated peridotites were also analyzed to obtain precise noble gas isotope compositions.

The halogens of all peridotites are heavily enriched in I, although the halogen ratios are distinctive in each locality. These high I/Cl ratios show a strong contribution of sedimentary pore fluids [2]. The noble gases except for He have the elemental and isotopic ratios similar to elementally fractionated atmospheric noble gases dissolved in seawater, which is probably equivalent to those dissolved in sedimentary pore fluids. The ³He/⁴He ratios are similar to that of the mantle and distinctly higher than the atmospheric ratio. This indicates that the fluids derived from subducting slabs acquired He from the ambient mantle, where He is much more enriched than in seawater.

These pore fluid-like halogen and noble gas signatures are strong evidence that the H₂O-rich fluids in the studied peridotites are derived from sedimentary pore fluids and transported to the mantle.

References: [1] Sumino *et al.* (2010) *EPSL* **294**, 163. [2] *e.g.* Muramatsu *et al.* (2007) *Appl. Geochem.* **22**, 534. [3] Kawamoto *et al.* (2013) *PNAS* **110**, 9663. [4] Ishimaru *et al.* (2007) *J. Petrol.* **48**, 395. [5] Arai & Hirai (1985) *Nature* **318**, 276.

キーワード: 水, ハロゲン, 希ガス, 沈み込み帯, マントル, かんらん岩
Keywords: water, halogen, noble gas, subduction zone, mantle, peridotite

東海地域におけるフィリピン海プレートの沈み込みに伴う温度場・脱水と想定東海地震・SSE・LFEとの関連性
Relations among temperature, dehydration of the PHS plate, and a large earthquake, a SSE, and LFEs in the Tokai district

末永 伸明^{1*}; 吉岡 祥一²; 松本 拓己³
SUENAGA, Nobuaki^{1*}; YOSHIOKA, Shoichi²; MATSUMOTO, Takumi³

¹ 神戸大・理, ² 神戸大・都市安全セ/理, ³ 防災科研

¹Graduate School of Science, Kobe Univ., ²RCUSS, Graduate School of Science, Kobe Univ., ³NIED

東海地域では、海溝型巨大地震の発生が懸念されており (e.g., Ishibashi, 1980)、浜名湖周辺では 2000 年から約 5 年にわたって長期的スロースリップイベント (SSE) が発生した (e.g., Miyazaki et al., 2006)。また、東海地方では深部低周波地震 (LFE) の震源の深さが東へ行くほど深くなる傾向がみられる。本研究では、東海地域において、フィリピン海プレートの沈み込みに伴う温度場の数値シミュレーションを行い、海洋地殻中の中央海嶺玄武岩 (MORB) の相図を用いてフィリピン海プレート上面からの脱水過程を見積もった。得られた温度場及び脱水過程の計算結果から、東海地震の想定震源域、浜名湖周辺で発生した長期的 SSE 及び東海地域における LFE の発生原因との関連についてそれぞれ考察した。計算モデルは 2 次元箱型熱対流モデル (Yoshioka et al., 2013) を使用し、駿河トラフを始点として東海地方を通る 3 本の平行な測線を設定し、それぞれの測線に沿った鉛直断面内の温度場を計算した。末永他 (2013 日本地震学会) からの主な変更点は、プレート境界面での摩擦熱を計算する際のパラメータである間隙水圧比について、一様な値から深さによって異なる値を与える改良を行った。その結果、計算結果の温度場の妥当性の指標となる地殻熱流量の観測値と計算値のフィッティングが改善され、その結果に基づき、プレート境界面の温度、プレート上面からの脱水過程について見直しを行った。プレート間カップリングがみられる上端・下端の深さは温度によって支配されると考えられており (Hyndman and Wang, 1993)、プレート境界面の温度 150~350 °C の領域を東海地震の想定震源域とすると、その深さの範囲は 9~21 km のプレート境界面となり、その領域は東へ行くにつれて狭くなった。また、浜名湖周辺の SSE 発生領域では、プレート境界面温度が 350~450 °C となり、不安定すべりから安定すべりへの遷移領域に相当した。また、SSE 発生領域付近では blueschist から greenschist への相転移に伴う脱水反応が生じ、プレート境界面に水が存在することが推定される。東海地域での LFE の震源分布域でのプレート境界面の温度は 500~630 °C とばらつきがみられたが、脱水過程をみると、greenschist から epidote amphibolite または blueschist から greenschist への相転移による脱水反応が震源分布域周辺でみられた。そこで本研究では、LFE の発生原因として、プレート境界面での水の存在が第一要因であるとし、震源の深さに差がみられるのは、異なる脱水過程を経るためにプレート境界面において水が存在する深さが東へ行くほど深くなっているためであると結論づけた。

キーワード: 2次元箱型熱対流モデル, 巨大地震, 低周波地震, スロースリップ, 温度, 脱水

Keywords: 2-D thermal modeling, megathrust earthquake, low-frequency earthquake (LFE), slow slip event (SSE), temperature, dehydration from hydrous MORB

四万十帯・室戸地域における CO₂ 流体の広域的分布・鉱物脈中の変化 The regional and single-vein scale distribution of the CO₂ fluids in the Shimanto accretionary complex, Muroto area, SW

武者 倫正^{1*}; 土屋 範芳¹; 岡本 敦¹
MUSHA, Michimasa^{1*}; TSUCHIYA, Noriyoshi¹; OKAMOTO, Atsushi¹

¹ 東北大学 環境科学研究科

¹ Environmental Studies of Tohoku University

Carbon dioxide and methane are major carbonic components of the fluids in the crust. The crustal fluids generally have composition of C-H-O system, mainly composed of H₂O, CO₂, and CH₄, and they may be carried down into Earth's interior at subduction zones. Many studies have examined fluid components in various accretionary prisms under low-grade metamorphic conditions, and CH₄ is showed as the only carbonic species. Therefore, there is little information on the variation of the components of C-H-O fluids in subduction zones.

The Tertiary (Paleogene and Neogene system) Shimanto belt, southwest in Japan, is one of the best-studied ancient accretionary complexes. The Muroto Peninsula belongs to the Tertiary Shimanto belt, and it is mainly composed of sandstones, mudstones and conglomerates with small amount of basalt. Mineral veins were mainly composed of quartz, with small amount of calcite near the vein walls, while many studies have showed CH₄ is the only carbonic component in the Shimanto belt, therefore it is unclear why calcite precipitated in the veins in absence of CO₂. Lewis (2000) reported the fluid inclusions of CH₄ and CO₂ mixture at one area in the Muroto Peninsula, but the extensive distribution of CO₂ fluids in the whole peninsula is not clear. In this study, we examined the distribution of C-H-O fluids from the Muroto Peninsula, as fluid inclusions in the mineral veins, using microthermometry and Laser Raman spectroscopy, in regional scale and single vein scale.

Fluid inclusions from quartz in the veins are composed of one-phase carbonic inclusions (only CH₄) and two-phase aqueous inclusions (carbonic vapor and H₂O liquid). Carbonic components of the vapor phase in the two-phase inclusions are gradually transitioned from CH₄-dominant in the north area of the belt to a CO₂?CH₄ mixture in the south; the CO₂/(CO₂ + CH₄) ratio in mole fraction (X_{CO_2}) vary from 0~0.3 in the north area to 0~0.9 in the south.

In single vein scale, we examined single CO₂-bearing vein from the south area of the Peninsula, where X_{CO_2} is 0~0.8. The CO₂ ratio in the carbonic species is decreased from the vein wall ($X_{CO_2} = 0.5?0.8$) to the vein center, in which carbonic species in the fluids is only CH₄ ($X_{CO_2} = 0$). The existence of CO₂ only near the vein walls is in good agreement of the precipitation of calcite near the vein walls. The homogenization temperature increases from ~180 °C to 240?250 °C, indicating the transition of the carbonic species from CO₂?CH₄ to CH₄ during vein formation.

The dominant species of carbonic species in most accretionary prisms is CH₄ under low-grade metamorphic conditions, and thermodynamic calculation about equilibrium in the C-H-O fluids also shows that CH₄ is dominant carbonic species in the equilibrium with graphite under the P?T conditions of formation of the CO₂-bearing veins (235?245 °C, 165?200 MPa). The CO₂-fluids are preferentially distributed close to an out-of-sequence thrust that brings the Muroto sub-belt into contact with the late Oligocene?early Miocene Nabae sub-belt with its many volcanic lavas and intrusive rocks. Therefore, the CO₂-fluids were considered to be magmatic-origin, and that the fluids were injected and mixed with the CH₄-pore-fluids of the sediments in the accretionary prism in the timing of formation of CO₂-bearing veins.

キーワード: 流体包有物, 付加体, 方解石, 鉱物脈, C-H-O 流体, 四万十帯

Keywords: fluid inclusions, accretionary complexes, calcite, mineral veins, C-H-O fluid, Shimanto belt

山口県徳佐盆地の地下における深部流体の流動 Visualization of deep-seated fluid flow in Tokusa Basin, Yamaguchi Prefecture

西山 成哲^{1*}; 田中 和広²; 鈴木 浩一³
NISHIYAMA, Nariaki^{1*}; TANAKA, Kazuhiro²; SUZUKI, Koichi³

¹ 山口大学, ² 山口大学, ³ 電力中央研究所

¹Yamaguchi University, ²Yamaguchi University, ³Central Research Institute of Electric Power Industry

わが国には、内陸部にも関わらず高塩濃度の地下水が湧出していることが知られており（酒井ほか，1978），流体の湧出箇所は地表からの自然湧水とボーリング孔からの湧水に区別される．深部流体は地下深部よりもたらされるため，その湧出箇所の特定は高レベル放射性廃棄物の地層処分場のサイト選定や評価において重要である．本研究ではボーリング孔からの深部流体の湧出が観測される，徳佐盆地において地質・地下水調査及びCSAMT法による比抵抗探査を行い，ボーリング掘削で確認された深部流体がどのように岩盤中を上昇し，被覆層が存在する場合，その後どのように流動するのかに関して検討を行った．

徳佐盆地内には白亜紀の溶結凝灰岩と流紋岩溶岩が分布し，これらを未固結の砂礫，粘土からなる更新統と完新統が覆っている．基盤岩中においては，徳佐-地福断層（佐川ほか，2008）に沿い，確認される範囲で約2.5kmの区間において低比抵抗帯が連続し，堆積物中においては断層の北側に低比抵抗帯が舌状に分布している．堆積物中の低比抵抗帯は地下水の水質分布の結果からNaCl型地下水を起源とすることが明らかとなった．また，ボーリング孔から湧出する高濃度地下水の比抵抗と物理探査により得られた比抵抗が整合的であることより，岩盤中の低比抵抗はこれら高塩濃度地下水の上昇を捉えているものと考えられる．以上より，徳佐盆地における深部流体は，徳佐-地福断層沿いに上昇し，被覆層に浸透した後，天水による希釈を受けながら河川方向に流動したものと考えられ，ボーリング孔からの湧水は断層沿いに連続的に湧出している可能性が示された．

キーワード: 深部流体, CSAMT法, 徳佐-地福断層, 地下水流動

Keywords: Deep-seated fluid, CSAMT method, Tokusa-Jifuku fault, Groundwater flow

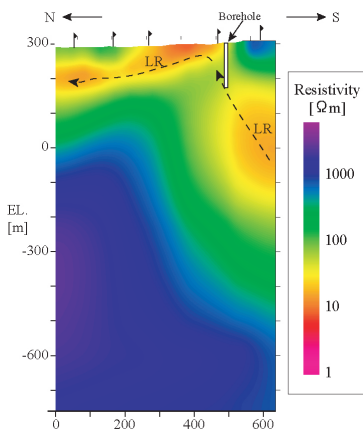


Fig.1 The resistivity profile by the CSAMT survey.

沈み込みプレート境界での非アスペリティの正体は粘土鉱物？ Can clay minerals account for the non-asperity on the subducting plate interface?

片山 郁夫^{1*}; 久保 達郎¹; 佐久間 博²; 河合 研志³
KATAYAMA, Ikuo^{1*}; KUBO, Tatsuro¹; SAKUMA, Hiroshi²; KAWAI, Kenji³

¹ 広島大学地球惑星システム学, ² 物質・材料研究機構, ³ 東京工業大学地球惑星科学

¹Department of Earth and Planetary Systems Science, Hiroshima University, ²National Institute for Materials Science, ³Department of Earth and Planetary Sciences, Tokyo Institute of Technology

沈み込みプレート境界面には、プレート間同士がしっかりと固着しているアスペリティと普段から安定的にすべる非アスペリティが分布し、プレート間地震はおもに前者のアスペリティで発生する。では、アスペリティと非アスペリティを作り出す原因はなんだろうか？アスペリティは空間的に不均質に分布するため温度圧力などによる鉱物の相転移を想定することは難しく、これまでは海山などの沈み込みによるプレート面での凸凹が有力視されている（例えば Cloos, 1992）。しかし、海山などの沈み込みが見られない地域や陸源性の堆積物によってプレート境界面が平滑にされている箇所にもアスペリティがみられ、その実体についてはまだ不明な点が多い。私たちは、アスペリティと非アスペリティの違いはプレート境界上に分布する物質の違いであるとの仮説をたて、粘土鉱物の摩擦特性に注目した実験を行なっている。摩擦の性質としては、速度を急変させた際の応答（速度依存性）から地震性すべりか非地震性すべりかが議論されることが多いが、今回は摩擦が静止（固着）した際に強度がどの程度回復するかを調べるヒーリング実験を行なった。これまでの予察的な実験の結果、スメクタイトと緑泥石は石英に比べ強度の回復が極端に小さいことが分かった。このことは、摩擦面に石英などの無水鉱物がある状態では固着強度が時間とともに回復するのに対し、粘土鉱物が分布する面上では固着力が弱く強度の上昇が妨げられる。プレート境界面では、沈み込むプレートから絞り出される水溶液により粘土鉱物が不均質に分布していることが考えられるため、アスペリティを囲う非アスペリティはそのような変質による粘土鉱物の存在によって生じるのかもしれない。

キーワード: プレート境界地震, アスペリティ, 粘土鉱物, 摩擦実験, 強度回復

Keywords: Interplate earthquake, Asperity, Clay minerals, Frictional experiment, Frictional healing

メルト包有物の硫黄化学状態から見た島弧初生マグマの酸素分圧 Oxidation state of arc primary magma-inferred from sulfur speciation of melt inclusions

清水 健二^{1*}; 柏原 輝彦¹; 為則 雄祐²
SHIMIZU, Kenji^{1*}; KASHIWABARA, Teruhiko¹; TAMENORI, Yusuke²

¹ 海洋研究開発機構, ² 高輝度光科学研究
¹JAMSTEC, ²JASRI, SPring-8

Oxidation state of arc magmas highly influences the chemical behaviors of redox sensitive elements such as chalcophile and some siderophile elements in subduction zone. Therefore, Oxidation state of arc magmas is essential to understand arc magma geneses and evolutions of ore deposits. It has been suggested that sub-arc mantle is oxidized by subducted materials such as fluid, sediments and oceanic crust. However, recent studies contradicted that the oxidation state of primary arc magma (sub-arc mantle) is similar to the average upper mantle and oxidation is caused by differentiation associated with crystallization and interaction within preexisting crust (e.g. Lee et al., 2012, *Science*, v336, p64).

In order to constrain oxidation state of primary arc magmas at an immature subduction zone, we have analyzed S₆₊/ΣS of boninitic and tholeiitic melt inclusions within Cr-spinel from Bonin Islands and Guam by soft X-ray microbeam at SPring-8/BL27SU. Boninite in Bonin Islands uniquely formed at the early stage of subduction formation (~50 Ma) by melting of highly depleted hydrous mantle and 0-7 myrs later, related arc tholeiites erupted in southern Bonin Islands and Guam by melting of depleted mantle (Ishizuka et al., 2011, *EPSL*, v306, p229). Compositions of melt inclusions fully cover compositional ranges of whole-rocks and some boninitic melt inclusions have MgO higher than 20 wt%, showing that they are very primitive magmas. S₆₊/ΣS of boninitic and tholeiitic melt inclusions are 0.57 to 0.78 and 0.47 to 1, respectively; S₆₊/ΣS of all high-MgO (7 to 12 wt%) tholeiitic melt inclusions are >0.9. Oxygen fugacities of primary boninite and tholeiite are estimated to be ΔFMQ >+1 and >+1.5, respectively by experimental results of Jugo et al. (2010, *GCA*, v74 p5926), indicating that sub-arc mantle is oxidized even at an early stage of subduction zone. Between the period of eruption of boninite and tholeiite, not only mantle sources but also the subducting component in term of oxidation state of sub-arc mantle may have changed.

キーワード: メルト包有物, ボニナイト, 島弧, 硫黄
Keywords: melt inclusion, boninite, arc, sulfur

Evaluating slab-fluid contribution into inhomogeneous mantle source: geochemical variation of Central and East Java arc Evaluating slab-fluid contribution into inhomogeneous mantle source: geochemical variation of Central and East Java arc

Handini Esti^{1*}; 長谷中 利昭¹; Wibowo Haryo Edi²; 柴田 知之³; MORI Yasushi⁴; HARIJOKO Agung²
HANDINI, Esti^{1*}; HASENAKA, Toshiaki¹; WIBOWO, Haryo edi²; SHIBATA, Tomoyuki³; MORI, Yasushi⁴; HARIJOKO, Agung²

¹Graduate School of Science and Technology, Kumamoto University, ²Geological Engineering, Gadjah Mada University, ³Institute for Geothermal Sciences, Kyoto University, ⁴Kitakyushu Museum of Natural History and Human History

¹Graduate School of Science and Technology, Kumamoto University, ²Geological Engineering, Gadjah Mada University, ³Institute for Geothermal Sciences, Kyoto University, ⁴Kitakyushu Museum of Natural History and Human History

The spatial distribution of the volcanoes in Central and East sections of Java arc denotes the widest and the narrowest of Java Island. Central Java section corresponds to the largest range and depth of Wadati-Benioff Zone along the island (180-360 km), whereas East Java section shows the narrowest range (190-220 km). However, both sections equally show wide geochemical variation with the function of slab-depth. Both also mark the appearance of the rear-arc alkaline suites in a different slab depth (360 km for Central Java, and 220 km for East Java). Geochemical datasets of basalt to basaltic andesite (further screened on Zr/Nb basis) from these sections were compiled to evaluate the contributions of slab-derived fluid to the mantle sources, and to assess the possible mantle sources of these magmas.

We group the lavas of the Central and East Java into two series: (1) the volcanic front series (VF), calc-alkaline suites of frontal- and middle-arc region volcanoes of Central and East Java, and (2) the rear-arc series (RA) consists of alkaline suites from Central and East Java (Muria, and Ringgit-Beser and Lurus, respectively). The VF series consistently shows typical island arc geochemistry, with strong LILE enrichment (Sr, Ba, Pb, and Rb) relative to HFSE. The RA series, mainly Muria, indicate stronger enrichment of LILE than other volcanoes closer to the trench. Ringgit-Beser and Lurus, the rear-arc lavas of East Java, behave differently in LILE enrichment. Ringgit-Beser lavas shows stronger LILE enrichment than that of lavas from Lurus, within the same enrichment range of Muria lavas. In the other hand, Lurus lavas are showing obvious HFSE depletion compared to OIB. The decreasing trend of LILE/HFSE and LILE/LREE (e.g. Ba/Nb, Ba/La, Pb/Ce, Pb/Nb) is observed across both Central and East Java sections. These ratios become lower toward the rear-arc of both sections, and the lowest in the rear-arc of Central Java. In various normalized plots (such as Nb vs. Ba/Nb), the VF series are plotted within the range of typical island arc basalts (IAB). Muria lavas, the rear-arc alkaline suite of the Central Java, resemble OIB and other non-arc type alkaline rock characteristics, but with positive indications of being island arc, such as negative Nb and Ti anomalies. Ringgit-Beser and Lurus alkaline lavas of East Java, however, are associated with other arc-type alkaline rock characteristics, with stronger signature of island arc than Muria.

Our analyzed samples show that lavas from East Java are closer in compositions to primitive magmas compared to Central Java's. The thicker overriding crust beneath Central Java than East Java possibly acts as the magma retainer that allows extensive fractionation. Across-arc variation of slab-derived fluid in both sections are observed as shown by decreasing LILE/HFSE and LILE/LREE toward rear-arc, suggesting the decreasing amount of slab-fluid added to the great slab-depth. The slab-fluid added to the volcanic front of East Java is slightly higher than that of Central Java, which may be controlled by the narrow range of slab dehydration area in the former that allows more fluid to concentrate. The low ratio of these trace elements in the rear-arc of both sections suggests that these parts have also been affected by dehydration of subducted slab. The stronger slab-fluid contributions in the rear-arc alkaline lavas of East Java than that of Central Java may reflect the role of shallower slab depth. Different mantle characteristics between the rear-arc of Central and East Java may reflect several possibilities: (1) the inhomogeneous mantle plume (E-type/EMI) beneath both sections, or (2) stronger EMI-type mantle contribution to Central Java than to East Java, or (3) the combination of both.

キーワード: Sunda arc, slab-derived fluid, across- and along-arc variations, trace elements
Keywords: Sunda arc, slab-derived fluid, across- and along-arc variations, trace elements

かんらん石-石英境界における熱水変質の反応進行度と空隙率変化 Reaction progress and porosity change in hydrothermal alteration at Olivine/Quartz boundary

大柳 良介^{1*}; 岡本 敦¹; 土屋 範芳¹
OYANAGI, Ryosuke^{1*}; OKAMOTO, Atsushi¹; TSUCHIYA, Noriyoshi¹

¹ 東北大学大学院環境科学研究科

¹ Graduate School of Environmental Studies, Tohoku University

Serpentinization in oceanic lithosphere is a fundamental process to bring water into deep earth's interior. It is known that silica activity controls the reaction paths during the hydrothermal alteration of peridotites [e.g. 1,2], however the detailed reaction mechanism induced by silica transport is poorly understood. In this study, we conducted hydrothermal experiments in olivine (Ol)-quartz (Qtz)-H₂O system for investigating the mechanism of silica metasomatism at crust/mantle boundary.

Composite powders, which was composed of Qtz zone and Ol zone was set in inner tubes, with diameters of 1.7 mm and heights of 50 mm, and then loaded into autoclave with alkaline solution (NaOH, aq, pH = 13.8 at 25 °C). Temperature and pressure are 250 °C and vapor-saturated pressure (= 3.98 MPa), respectively. After the experiments, the inner tube was cut into ten segments to evaluate the reaction progress as a function of the distance from Ol/Qtz boundary (hereafter denoted X), by Thermogravimetry and XRD. In order to evaluate the spatial variation of the reactions, the area of each minerals (olivine and reaction products) and pore was measured from the back-scattered electron (BSE) images of the thin section.

After 46 days, the H₂O content near the Ol/Qtz boundary is lower (3.9 wt.% H₂O) than that in (12 wt.%) at the margin of the reaction tube. The reaction products after olivine changed systematically as away from Ol/Qtz boundary from smectite+serpentine zone to the serpentine+brucite zones. In the smectite+ serpentine zone, the (Mg+Fe)/Si ratio of the products increases from 0.5 to 1.5, indicating that proportion of serpentine with respect to smectite increased away from the boundary. With increasing time, the smectite+ serpentine zone was enlarged, where as the serpentine+brucite zones was retreated.

Based on the combined analyzes of BSE images, TG and SEM-EDS, we obtained the reaction progresses of individual elementary reactions between 25 and 46 days as follows:

(1) In the smectite+ serpentine zone, smectite was formed via hydration of olivine and dehydration of serpentine by supply of silica. As the result, overall reaction has a variation in the smectite+ serpentine zone; Δm_{H_2O} is negative (hydration) at X=0-4 mm, it is positive (dehydration) at X=4-10 mm. Volume expansion factor (V/V_0) is much higher (=1.4) at Ol/Qtz boundary than other zones (~ 1.1), mainly due to Si-metasomatic reaction.

(2) Far from the Ol/Qtz boundary (X = 20-40 mm), there is no influence of silica supply, indicating that silica was completely consumed in the smectite+ serpentine zone. In these area, serpentinization proceeds as the typical olivine hydration reaction to produce brucite and serpentine with constant Srp/Brc ratio.

(3) In the transient zone, serpentine was formed by two ways: hydration of olivine and dehydration of brucite by supply of silica. These two serpentine forming reaction resulted in a large amount of serpentine in this area, and high volume expansion factor (~ 1.4).

Due to these two volume expansion reactions, low porosity ($\sim 5\%$) area developed locally, never-theless porosity of other area is 30%. The amount of silica ($\Delta m_{SiO_2, aq}$), which consumed from 25 to 46 days, is largest at Ol/Qtz boundary, and monotonically decreases with increasing distance. If excess silica are available, the zones affected by silica will increase gradually with increasing time during hydrothermal alteration around mantle/crust boundary. In contrast, the porosity has a minimum around X = 15 mm in the transition zone, because Ol-hydration and Brc-dehydration reaction proceed with large volume expansion. Such volume expansion reaction and mineral changes causes the mechanical strength of boundary.

References:

- [1] Frost, B. R., & Beard, J. S. (2007). *Journal of Petrology*, 48(7), 1351-1368.
- [2] Ogasawara, Y., Okamoto, A., Hirano, N., & Tsuchiya, N. (2013). *Geochimica et Cosmochimica Acta*, 119, 212-230.

Keywords: serpentinization, ultramafic rock, Si-metasomatism, Hydrothermal alteration

沈み込み帯におけるメルトの分布と輸送 Distribution and transportation of melt in subduction zones

石井 和彦^{1*}
ISHII, Kazuhiko^{1*}

¹ 大阪府立大学大学院理学系研究科
¹ Graduate School of Sciences, Osaka Prefecture University

沈み込み帯で起こる地震・火山活動や変成作用を総合的に理解するために、地球物理学的・岩石学的な実験・観測・解析のほか、それらから得られる多様な情報を相互に関連づける様々な数値モデリングが行われている。しかし、沈み込み帯ではスラブやマントルウェッジの脱水・加水・溶融・固結に加え、流体の移動や流体による粘性の変化（部分溶融・加水軟化）など、様々な過程が相互に関連しながら起こるため、各過程を個別にではなく総合的に理解する必要がある。本研究では、スラブの脱水、マントルウェッジの加水・脱水、マントルウェッジの部分溶融、メルトとH₂O流体の移動、温度・含水量・部分溶融度に依存したかんらん岩の流動則を考慮した数値モデルを用いて計算を行った。このモデルでは、地震波トモグラフィーなどの結果から推定されている、火山フロントの下からマントルウェッジ内にスラブとほぼ平行に延びるメルトの分布を再現することができるが、その形状はかんらん岩に対する水の溶解度、およびメルトやH₂O流体の浸透流速度などのパラメータに依存して変化する。発表では、メルトの分布に対するこれらのパラメータの効果について検討し、沈み込み帯で起こる諸過程の相互関係について議論する。

キーワード: 沈み込み帯, メルト, 分布と輸送
Keywords: subduction zones, melt, distribution and transportation

鉱物の粒径分布が及ぼすマントルウェッジ内の水の流動パターン Effects of mineral grain size variation on fluid migration in the mantle wedge

和田 育子^{1*}; Behn Mark D.²
WADA, Ikuko^{1*}; BEHN, Mark D.²

¹ 東北大学災害科学国際研究所, ² ウッズホール海洋研究所
¹IRIDeS, Tohoku University, ²Woods Hole Oceanographic Institution, USA

In this study, we investigate the effect of mineral grain size on the migration paths of aqueous fluids in the mantle wedge. Grain size is an important parameter that controls the grain-scale permeability of the mantle; in general, the smaller the grain size, the less permeable the mantle is, provided that the pores between grains are connected. The migration paths of aqueous fluids are therefore dependent on the grain size distribution, influencing the location and the degree of hydrous melting in the mantle wedge and the location of arc volcanism. We develop a 2-D fluid migration model with generic subduction zone geometry. In the model, we adopt grain size distributions calculated by coupling a subduction zone thermal model with a laboratory-derived grain size evolution model for a range of subduction parameters (Wada et al., 2011). The fluid migration model also includes the effects of mantle flow velocities and mantle-flow-induced pressure gradients, both of which are also calculated from the thermal model. The calculated grain size immediately above the slab is on the order of 10²-100 μ m beneath the forearc region, depending on the slab thermal structure, and it increases down-dip to a few cm beneath the arc region. Our preliminary modeling results with a simplified fluid influx pattern indicate that the aqueous fluids tend to become trapped in the down-going mantle due to low permeability and dragged down-dip until permeability becomes high enough for the fluids to migrate upward. Grain size above a colder slab tends to be smaller than that above a warmer slab, and therefore fluids become dragged down-dip further in a cold-slab subduction zone than in a warm slab subduction zone. A colder slab also tends to release fluids at deeper depths than a warmer slab, influencing the pattern of fluid influx into the mantle wedge. In this study, we calculate the fluid influx along the base of the mantle wedge, using the thermal modeling results and thermodynamic calculations based on *Perple_X*, and quantify fluid migration in the mantle wedge with the grain size and fluid influx distributions that are consistent with a given slab thermal structure.

キーワード: subduction zone, mantle wedge, aqueous fluid migration, grain size, slab dehydration, arc volcanism
Keywords: subduction zone, mantle wedge, aqueous fluid migration, grain size, slab dehydration, arc volcanism

圧力 1GPa におけるアンチゴライト蛇紋岩弾性波速度の温度依存性 Temperature dependence of seismic velocities in a antigorite serpentinite at 1 GPa

白井 亮^{1*}; 渡辺 了¹; 米田 明²; 道林 克禎³

SHIRAI, Ryo^{1*}; WATANABE, Tohru¹; YONEDA, Akira²; MICHIBAYASHI, Katsuyoshi³

¹ 富山大学理学部地球科学科, ² 岡山大学地球物質科学研究センター, ³ 静岡大学理学部地球科学科

¹Department of Earth Sciences, Faculty of Science, University of Toyama, ²Institute for Study of Earth's Interior, Okayama University, ³Institute of Geosciences, Shizuoka University

Serpentines play key roles in subduction zone processes including water transport, seismogenesis, exhumation of high-pressure rocks, etc. Geophysical mapping of serpentinitized regions in the mantle wedge leads to further understanding of these processes. Seismic properties of serpentinitized peridotites are critical to interpretation of seismological observations. Antigorite is a major form of serpentine, which is stable to higher temperatures. The single-crystal elastic properties were recently revealed via Brillouin scattering technique (Bezacier et al., 2010; 2013). However, the temperature dependence of elastic properties is still poorly understood. We have measured elastic wave velocities in a antigorite serpentinite at high temperature and pressure conditions.

A black massive antigorite serpentinite was collected from the Nagasaki metamorphic rocks, western Japan. It is composed of antigorite (98.0 vol.%), diopside (1.5 vol.%) and magnetite (0.5 vol.%). Microstructural observation reveals an interpenetrating texture characterized by randomly oriented antigorite blades. Antigorite CPO data shows weak concentration of antigorite axes. Elastic wave velocities measured at 180 MPa shows very weak anisotropy in elasticity. Cylindrical samples (D=L=6mm) were made with ultrasonic machining.

Measurements were made at the pressure of 1 GPa and the temperature of up to 550 C, by using a piston-cylinder type high pressure apparatus at ISEI, Okayama University. The pulse reflection technique was employed for velocity measurement. One LiNbO₃ transducer with the resonant frequency of 5 MHz was used to transmit and receive ultrasonic signals. The length of the sample at high pressure and temperature conditions was estimated from the length of the recovered sample.

Both compressional and shear wave velocities linearly decrease with increasing temperature. The temperature derivatives are -3.6×10^{-4} (km/s/K) and -2.7×10^{-4} (km/s/K) for compressional and shear wave velocities, respectively. The temperature derivative of compressional wave velocity is close to that observed in the direction subparallel to antigorite *c*-axis (Yano et al., in prep.). The temperature dependence of *c*₃₃ might dominate that of the effective elastic constants of a randomly oriented polycrystalline aggregate. Applications to seismological observations will also be discussed in this presentation.

キーワード: 地震波速度, 蛇紋岩, アンチゴライト, 沈み込み帯, 流体

Keywords: seismic velocity, serpentinites, antigorite, subduction zone, fluid

ラマン・赤外分光計測による石英表面の水の構造化の検出とその分子動力学的評価 Detection of structured water on quartz interface by Raman-FTIR spectroscopy and its evaluation by molecular dynamics

石川 慧^{1*}; 佐久間 博²; 土屋 範芳¹
ISHIKAWA, Satoru^{1*}; SAKUMA, Hiroshi²; TSUCHIYA, Noriyoshi¹

¹ 東北大学大学院環境科学研究科, ² 独立行政法人 物質・材料研究機構

¹ Graduate School of Environmental Studies, Tohoku University, ² National Institute for Materials Science

地殻中では含水鉱物や流体包有物中の水、間隙中の水など、様々な形で水が存在しており、プレートの沈み込み帯も、海洋由来の水やマントル由来の水などが存在する環境である。沈み込み帯における地震発生帯の温度は 150~350 °C 程度であり、水は亜臨界-超臨界で存在する熱水である。また、この領域の水は鉱物粒界に非常に薄い薄膜状の形で存在しており、この薄膜水はバルクの水（自由水）とは違った性質を持つことが知られている。

本研究では、高温高压の薄膜水が観察可能なダイヤモンドセルと顕微ラマン-赤外分光計を用いて、様々な温度圧力における金属反射板上および石英基板上の水を観察した。

ラマンスペクトルおよび赤外吸収スペクトルの観察結果より、3400cm⁻¹ 付近に現れる水の OH 伸縮振動ピークが温度圧力によって変化することが観察された。このピークは高温では水素結合の影響は弱まり 3700cm⁻¹ 付近にシフトするが、石英基板上の水について、高温であっても水素結合の影響を強く受けた 3200cm⁻¹ 付近の振動の存在が確認された。

また本研究では、分子動力学プログラム MXDORTO を用いて実験を模擬した条件でシミュレーションを行い、石英基板上の水の構造化を再現した。シミュレーションでは、石英表面近傍の数ナノメートルの範囲において、通常の水には見られない水の密度の分布が見られた。

以上のような分光観察、分子シミュレーションを用いて得られた石英表面の水分子の構造および性質の変化を、水分子と石英表面のシラノール基 (Si-OH) の水素結合に着目して考察する。

キーワード: ラマン分光, 赤外分光, 界面水, 亜臨界, 石英, 分子動力学

Keywords: Raman spectroscopy, IR spectroscopy, interfacial water, subcritical, quartz, molecular dynamics

地質学的証拠に基づいた地殻流体が関与する岩石破壊過程の解明 Generation process of brecciated marble at Hiraodai karst, Kyushu, Japan

石山 沙耶^{1*}; 安東 淳一¹; 中井 俊一²; 太田 泰弘³; ダス カウシク¹
ISHIYAMA, Saya^{1*}; ANDO, Jun-ichi¹; NAKAI, Shun'ichi²; OTA, Yasuhiro³; DAS, Kaushik¹

¹ 広島大学理学研究科地球惑星システム学専攻, ² 東京大学地震研究所, ³ 北九州市立自然史・歴史博物館いのちのたび博物館

¹Department of Earth and Planetary Systems Science, Hiroshima University, ²Earthquake Research Institute, the University of Tokyo, ³Kitakyushu Museum of Natural history & Human history

Geofluid is believed to be closely related to the seismic and volcanic activities. However, the detail relationship of geofluids with seismicity and volcanic activity is not studied properly through geological observations. We have found recently the brecciated marble widely distributed at Hiraodai karst plateau, Fukuoka Pref. This brecciated marble offers unique opportunity to study the relationship between geofluid and seismicity. Here, we shall explore the generation process of this brecciated marble through geological, microstructural and geochemical methods using polarization microscope, SEM, TEM, EPMA, microthermometric and MC-ICP-MS techniques.

The marble in Hiraodai karst plateau was thermally metamorphosed due to Cretaceous Hirao granodiorite intrusion. The brecciated marble occupies about 0.7 km x 1km of area in the central part of the karst. The main results of the present study are as follows.

- 1) The brecciated marble is composed of the rock fragments with variety of sizes ranging from millimeter to meter scale, and having angular to rounded shapes.
- 2) Numerous fluid inclusions are observed in the thin section of the brecciated marble.
- 3) TEM observation shows that the dense tangled dislocations are formed in calcite grains of the brecciated marble.
- 4) The homogenization and freezing temperatures of the fluid inclusions are about 240 deg C and 0 deg C, respectively.
- 5) The whole-rock and mineral separates (biotite and plagioclase) of Hirao granodiorite yields Rb-Sr isochron age of 129.4 +/- 2.4 Ma. Interestingly, Rb-Sr data of the fluid inclusions also lie on the Rb-Sr isochron of Hirao granodiorite.

The above-mentioned results of 1) and 2) suggest that the brecciation occurred by fluid infiltration and that the fragments were moved and rotated at very high speed. The result 3) demonstrates that the calcite grains of the brecciated marble experienced high stress. These three results together indicate that the brecciation process might generate seismic wave. On the other hand, the results of 4) and 5) suggest that the possible origin of the fluid inclusion is the released fluid from the Hirao granodiorite magma. Therefore, the brecciation of marble distributed at Hiraodai karst plateau was probably generated by magmatic fluid from Hirao granodiorite under high stress condition at 129.4 +/- 2.4 Ma ago.

Keywords: Brecciated rock, Hiraodai karst, Hirao granodiorite, Fluid inclusion, Rb-Sr isotope

沈み込む堆積岩層中の含水相 topaz-OH の高温高压下における状態方程式の決定 Equation of state of topaz-OH in the subducted sediment under high pressure and high temperature

新里 美月^{1*}; 井上 徹²; 蔡 闊²; 末次 秀規²; 柿澤 翔²

NIIZATO, Mizuki^{1*}; INOUE, Toru²; CAI, Nao²; SUENAMI, Hideki²; KAKIZAWA, Sho²

¹ 愛媛大学理学部地球科学科, ² 愛媛大学地球深部ダイナミクス研究センター

¹Department of Earth Sciences, Ehime University, ²Geodynamics Research Center, Ehime University

沈み込むスラブ中の含水鉱物の脱水分解反応によって H₂O に富んだ流体が生成され、その流体はマグマの生成や熔融温度の低下、マグマ組成の変化を引き起こすと考えられている。topaz-OH [Al₂SiO₄(OH)₂] は沈み込むスラブの堆積岩層中に存在すると考えられる含水鉱物であり、天然の topaz [Al₂SiO₄(OH,F)₂] の端成分である。安定領域については topaz-OH は 5-10 GPa、1500 °C まで安定に存在すると報告されている (Wunder *et al.*, 1993; Ono, 1998; Schmidt *et al.*, 1998)。状態方程式の研究は天然の topaz (Komatsu *et al.*, 2003; Gatta *et al.*, 2003) では行われているが topaz-OH においては未だに報告されておらず、また高温及び高压下での実験も行われていない。従って、本研究では topaz-OH の状態方程式すなわち熱弾性的性質を明らかにするために高温高压下での X 線その場観察実験を行った。

出発物質の topaz-OH はマルチアンビル型高压発生装置を用いた急冷回収実験によって 10 GPa、~1000 °C の条件下で合成した。X 線その場観察実験は高エネルギー加速器研究機構、PF-AR NE5C の高压発生装置 MAX80 を使用し、エネルギー分散法により X 線回折パターンの収集を 3-10 GPa、800 °C までの範囲で行った。熱弾性物性値は Angel (2000) による EosFit v5.2 の計算ソフトを用いて計算し、フィッティングには 3 次のバーチマーナハンの状態方程式を用いた。

高温高压条件下で得られた全データを 3 次のバーチマーナハン状態方程式によってフィッティングしたところ ($K'=4$ で固定)、 $V_0=354.7(1) \text{ \AA}^3$ 、 $K_0=169.8(22) \text{ GPa}$ 、 $(dK_T/dT)_P=-0.013(7) \text{ GPaK}^{-1}$ 、 $a_0=1.61(23) \times 10^{-5} \text{ K}^{-1}$ 、 $b_0=1.36(41) \times 10^{-8} \text{ K}^{-2}$ という値が得られた。一方、今回得られた圧縮データを詳しく解析すると、7 GPa 付近で圧縮特性の変化が示唆された。この現象は a 軸と b 軸の圧縮特性の変化として現れている。従って、7 GPa 付近を境界に低圧側、高压側で状態方程式の計算を試みた ($K'=4$ で fix)。結果、低圧側で $V_0=355.2(1) \text{ \AA}^3$ 、 $K_0=160.1(2) \text{ GPa}$ 、高压側で $V_0=356.5(9) \text{ \AA}^3$ 、 $K_0=153.1(89) \text{ GPa}$ と異なる値をとる結果が得られた。天然の topaz を用いた先行研究との比較を行うと本研究によって得られた topaz-OH の体積、体積弾性率はともに先行研究より大きい値となった。これは OH の含有量の増加に伴う体積弾性率の増加が原因であると考えられる。体積弾性率に対する密度の比較を行うと、topaz-OH はバーチの法則に従う直線近くに位置し、高压含水相である Ph D [Mg₂SiO₄(OH)₂] と並んで体積弾性率が大きく、密度が大きい鉱物であることが明らかとなった。そのため、topaz-OH は堆積岩層中の安定な領域ではスラブの沈み込みを促進させ、より深部へ水を運搬することができると思われる。

キーワード: topaz-OH, 高压含水相, 沈み込むスラブ, 状態方程式, 放射光 X 線その場観察

Keywords: topaz-OH, high pressure hydrous phase, subducting slab, equation of state, synchrotron X-ray in-situ experiment

メルト包有物と斜長石の Anorthite 成分から見積もる東北日本・伊豆弧の玄武岩質マ
グマの含水量
Water content in arc basaltic magma in northeast Japan and Izu-Mariana arc estimated
from melt inclusions in olivine and

潮田 雅司^{1*}; 池口 直毅¹; 高橋 栄一¹
USHIODA, Masashi^{1*}; IKEGUCHI, Naoki¹; TAKAHASHI, Eiichi¹

¹ 東京工業大学理工学研究科地球惑星科学専攻
¹Dept. Earth and Planetary Sciences, Tokyo Institute of Technology

Primitive arc basalt magma is generated by partial melting of sub-arc mantle with adding aqueous fluid which was derived from dehydration of subducting slab. Aqueous fluid has profound effects on melting temperature of the mantle, crystallization pathways of generated magmas, and explosivity of magmas. Precise estimation of H₂O content in arc basalt magma is important to evaluate the effect of water on generation, differentiation, and eruption of magmas in subduction zones. We estimated variation of water content of arc basaltic magmas in the northeast Japan arc and the Izu-Mariana arc using a simple plagioclase phenocryst hygrometer and melt inclusion analysis of olivine phenocrysts.

A simple plagioclase phenocryst hygrometer was constructed by high-pressure and high temperature experiments using internally heated pressure vessels: SMC-2000 and SMC-5000 installed at the Magma Factory, Tokyo Tech (Ushioda et al., 2013, VSJ fall meeting). High-pressure and high-temperature experiments were conducted for relatively primitive basalt from Miyakejima volcano under hydrous conditions. OFS (Ofunato scoria: Tsukui et al., 2001; Niihori et al., 2003) is one of the most primitive basalt in the last 10,000 years. All experiments were conducted near the liquidus of plagioclase (\pm magnetite) and therefore the composition of melt is essentially the same as the starting material. H₂O content of melt was calculated by weight ratio of melt using mass balance calculation of all phases assuming that water was concentrated only in melt. Partition coefficient $K_D^{pl-melt}_{Ca-Na}$ is proportional to H₂O content in melt. In the experimental conditions, both pressure and temperature effects are negligible.

We then chose geochemical data sets of relatively primitive basaltic rocks (with no evidence of magma mixing) and most frequent Ca-rich plagioclase phenocrysts from 15 arc basaltic volcanoes, which includes both frontal arc volcanoes and rear-arc volcanoes from literature. In 15 volcanoes, plagioclase phenocrysts of high anorthite content (An>90) are commonly observed, whereas plagioclase phenocrysts in rear arc volcanoes usually have lower anorthite content (90>An>80). Estimated H₂O content of basaltic magma is 3 wt.% H₂O or higher.

We also analyzed H₂O content of melt inclusions in olivine phenocrysts using FTIR micro reflectance measurement (Yasuda, 2011) and FTIR micro transmission measurement (absorption coefficient: Yamashita et al., 1996) in order to compare H₂O content between melt inclusion analysis and this simple plagioclase phenocryst hygrometer. For example, melt inclusions of olivine phenocrysts in scoria from Ko-Fuji volcano had up to 3.7 wt.% H₂O which was consistent with estimate from our simple plagioclase phenocrysts hygrometer. In Miyakejima volcano, melt inclusions of olivine phenocrysts from OFS contained up to 3.3wt.% H₂O although H₂O content was 5.2 wt.% estimated from this hygrometer. In either case, basaltic magmas in volcanic front have 3 wt.% H₂O or higher.

キーワード: マグマ中の水, メルト包有物, 斜長石メルト間平衡
Keywords: water in magma, melt inclusion, equilibrium between plagioclase and melt

加水・脱水反応に起因するフラクチャーパターン：個別要素法によるアプローチ DEM simulation on fracturing induced by hydration and dehydration reactions

岡本 敦^{1*}; 清水 浩之²
OKAMOTO, Atsushi^{1*}; SHIMIZU, Hiroyuki²

¹ 東北大学大学院環境科学研究科, ² 東北大学流体科学研究所

¹Graduate School of environmental Studies, Tohoku University, ²Institute of Fluid Science, Tohoku University

Dehydration and hydration reactions play significant roles on the global water circulation in the solid Earth, and cause drastic change in the mechanical properties of the subduction zone interface. Progress of both reactions requires an effective transport of water (release or supply) between the reaction sites and outer system, and are commonly characterized by large changes in solid volume, porosity, and fluid pressure. Reaction textures with fracturing are commonly observed both in hydration and dehydration hydration reactions. However, the dynamic relationship among reactions, fluid transport and deformation (fracturing, plastic deformation) is too complicated to be understood solely by observations of natural occurrences.

In the present study, we carried out numerical simulations on fracturing induced by hydration or dehydration reactions by using distinct element method (DEM). At first, we consider a dehydration reaction like a dehydration of serpentine. In the model, the following factors are introduced: (1) pressure dependence of reaction rate, (2) grain boundary as weak and water-saturated region, and that (3) mineral grains become permeable after fracturing or reacted. In this model, reaction rate drastically decreases with progress of dehydration reaction, when fluid cannot escape from the system.

We examined two rock systems; one is composed of reactive minerals (uniform-reactive system) and the other one is composed of reactive minerals embedded in unreactive matrix minerals (reactive minerals in matrix system). In both systems, one is drain-boundary, whereas all the others are undrain-boundary. The spatial variation in fractures and progress of reactions are contrasting between the two systems. In the uniform-reactive system, fracturing does not occur and reactions uniformly occur from the drain-boundary, because fluid effectively escapes through newly-produced pore-network. In contrast, the reactive-mineral-in-matrix-system, the fracture network is produced among the reactive grains, and heterogeneous distributions of reaction progress was produced in the rocks. We will further discuss the key parameters to controls the fracture patterns and difference between hydration and dehydration reactions.

Keywords: hydration, dehydration, fracturing, distinct element method